CD44 Variant Isoforms Promote Metastasis Formation by a Tumor Cell-Matrix Cross-talk That Supports Adhesion and Apoptosis Resistance

Pamela Klingbeil,[1] Rachid Marhaba,[1] Thorsten Jung,[3] Robert Kirmse,[2] Thomas Ludwig,[2] and Margot Zöller[1,3,4]

[1]Department of Tumor Progression and Immune Defense and [2]Section Microenvironment of Tumor Cell Invasion, German Cancer Research Center; [3]Department of Tumor Cell Biology, University Hospital of Surgery, University of Heidelberg, Heidelberg, Germany and [4]Department of Applied Genetics, University of Karlsruhe, Karlsruhe, Germany

Abstract

CD44 designates a large family of proteins with a considerable structural and functional diversity, which are generated from one gene by alternative splicing. As such, the overexpression of CD44 variant isoform (CD44v) has been causally related to the metastatic spread of cancer cells. To study the underlying mechanism, stable knockdown clones with deletion of exon v7 containing CD44 isoforms ($CD44v^{kd}$) of the highly metastatic rat adenocarcinoma line BSp73ASML ($ASML^{wt}$) were established. ASML-$CD44v^{kd}$ clones hardly form lung metastases after intrafootpad application and the metastatic load in lymph nodes is significantly reduced. Rescuing, albeit at a reduced level, CD44v expression in ASML-$CD44v^{kd}$ cells (ASML-$CD44v^{rsc}$) restores the metastatic potential. The following major differences in $ASML^{wt}$, ASML-$CD44v^{kd}$, and ASML-$CD44v^{rsc}$ clones were observed: (*a*) $ASML^{wt}$ cells produce and assemble a matrix in a CD44v-dependent manner, which supports integrin-mediated adhesion and favors survival. This feature is lost in the ASML-$CD44v^{kd}$ cells. (*b*) CD44v cross-linking initiates phosphatidylinositol 3-kinase/Akt activation in $ASML^{wt}$ cells. Accordingly, apoptosis resistance is strikingly reduced in ASML-$CD44v^{kd}$ cells. The capacity to generate an adhesive matrix but not apoptosis resistance is restored in ASML-$CD44v^{rsc}$ cells. These data argue for a 2-fold effect of CD44v on metastasis formation: CD44v-mediated matrix formation is crucial for the settlement and growth at a secondary site, whereas apoptosis resistance supports the efficacy of metastasis formation. (Mol Cancer Res 2009;7(2):168–79)

Introduction

The lymphocyte homing receptor CD44 attracted considerable interest, when it was described that CD44 splice variants (CD44v) suffice to confer a metastatic phenotype to locally growing tumor cells (1). Meanwhile, there is ample evidence for the importance of CD44v in tumor progression (2, 3). In addition, CD44 has been recognized as a cancer-initiating cell (CIC) marker in several types of cancer (4, 5). Notably, CIC are supposed to act as initiators of metastatic spread (4, 6). In view of the rather ubiquitous expression of CD44, its definition as a CIC marker may seem surprising. Yet, CD44 molecules vary considerably by *N*- and *O*-glycosylation and by insertion of alternatively spliced variable exon products in the extracellular domains of the molecule (7, 8). A multitude of isoforms is generated this way, which correspond to a multitude of functions (reviewed in refs. 2, 3, 9, 10). Indeed, the functional activities ascribed to CD44 could cover many activities required for metastasizing tumor cells.

First, CD44 is involved in several aspects of adhesion and motility (11). The major ligand of CD44 is hyaluronan (10, 12). Hyaluronan-bound CD44 interacts with actin via ankyrin (13) or activated ERM proteins (14). The CD44 interaction with the cytoskeleton can also proceed through Src kinases, Ras, and Rho GTPases (15). Peritumoral hyaluronan binding to CD44 on endothelial cells supports extravasation of tumor cells (16). Attachment can be strengthened by the association of CD44 with integrins (17) and may involve the CD44v6 isoform (18). CD44v also binds P- and L-selectin, which can promote the hematogenous spread of tumor cells (18). By hyaluronan binding, CD44 also can contribute to tumor invasiveness by stimulating the production of matrix metalloproteinase-2 and -9 (19). In addition, binding of matrix metalloproteinase-9 to the ectodomain of CD44 facilitates transforming growth factor-β processing and angiogenesis (20).

Second, CD44 can promote tumor cell proliferation (10). One pathway proceeds via CD44 interaction with neighboring transmembrane receptor tyrosine kinases, such as the ErbB family (21). Interactions can be direct or via the recruitment of

Received 4/28/08; revised 9/16/08; accepted 10/13/08; published OnlineFirst 02/10/2009.

Grant support: Mildred-Scheel-Stiftung für Krebsforschung, Tumorzentrum Heidelberg/Mannheim, and SPP1190 (M. Zöller).

The costs of publication of this article were defrayed in part by the payment of page charges. This article must therefore be hereby marked *advertisement* in accordance with 18 U.S.C. Section 1734 solely to indicate this fact.

Note: Supplementary data for this article are available at Molecular Cancer Research Online (http://mcr.aacrjournals.org/).

Current address for P. Klingbeil: Breakthrough Breast Cancer Research Centre, The Institute of Cancer Research, London, United Kingdom.

Requests for reprints: Margot Zöller, Department of Tumor Cell Biology, University Hospital of Surgery, University of Heidelberg, Im Neuenheimer Feld 365, D-69120 Heidelberg, Germany. Phone: 49-6221-565146; Fax: 49-6221-565199. E-mail: m.zoeller@dkfz.de

doi:10.1158/1541-7786.MCR-08-0207

matrix metalloproteinases by the heparan sulfate chain of CD44v3 (21, 22) and can depend on CD44v expression, such as the c-Met activation by CD44v6-bound scatter factor (23). In addition, CD44v6 ligation also can initiate activation of the mitogen-activated protein kinase pathway, thereby directly promoting tumor cell proliferation (24).

Third, CD44 supports cell survival. CD44 ligation supports anchorage-independent growth and apoptosis resistance, which both can proceed via activation of the phosphatidylinositol 3-kinase (PI3K)/Akt pathway (25) through the adaptor protein GAB1, such that focal adhesion kinase and BAD become phosphorylated (26). Besides this major pathway, osteopontin binding via CD44 provides a strong survival signal through integrin activation (27). There is evidence for engagement particularly of CD44v7 in the activation of antiapoptotic pathways (28).

The pancreatic adenocarcinoma BSp73ASML (ASML) is a highly metastatic tumor cell line. It metastasizes via the lymphatic system, such that animals succumb with lymph node and miliary lung metastases with no or minor local tumor growth (29). The latter feature allows surveillance of metastasis formation without any surgical intervention that might *per se* provide an unspecific stimulus on metastatic growth. One of the molecules selectively expressed by this metastasizing cell line, which is absent in a nonmetastatic subline of the same tumor (AS), was identified as CD44v. Transfection of the non-metastatic subline AS with CD44v4-v7 (AS-14) or CD44v6 but not CD44s cDNA promoted metastasis formation (1). However, metastasis formation by AS-14 differs from that by ASML cells inasmuch as AS-14 cells still grow locally at the injection site and form few, large metastatic nodules, whereas ASML cells form thousands of miliary metastases. Because ASML and AS cells do not only differ with respect to CD44v expression (30, 31), we considered a selective knockdown of CD44v4-v7 in ASML cells, an ideal model to evaluate which of the multiple functions ascribed to CD44 contribute to metastasis formation in this cell line.

Our data provide convincing evidence that (*a*) a CD44v-mediated production of an adhesive matrix is indispensable for a cancer cell's cross-talk with its microenvironment and (*b*) a CD44v-induced activation of antiapoptotic signaling contributes to the efficacy of metastatic settlement.

Results

Generation of ASML-CD44v^{kd} Cells and Morphologic Characterization

To define the effect of CD44v isoform expression on the lymphatic spread of highly metastatic ASML cells at the molecular level, we established a selective knockdown of alternatively spliced exon products by transfection with a v7-specific RNA interference (RNAi) expression plasmid, because CD44v4-v7 and CD44v6/v7 are the two most abundant CD44 isoforms in ASML cells (1). Western blot analysis using a CD44v6-specific antibody (no rat CD44v7-specific antibody is available) revealed efficient down-regulation of CD44v4-v7 and CD44v6/v7. Minor isoforms expressed by ASML are CD44s and v8-v10 (23, 32). As shown by reverse transcription-PCR (RT-PCR), these species are not affected by the v7 knockdown, whereby the RT-PCR product amplified with the CD44v8 primer corresponds according to its length to a CD44v8-v10 product (23, 32). This isoform is too weakly expressed to be seen after amplification with the CD44s primers, which reveal three bands, corresponding in size to CD44s, CD44v6/v7, and CD44v4-v7. The latter two bands as well as the band for v4 to v7 primers are strongly reduced in the CD44v7 knockdown. From the CD44v7 knockdown clones, rescue clones (ASML-CD44v^{rsc}) with restored CD44v4-v7 or CD44v6/v7 expression were generated. The constructs, protein, and mRNA expression as revealed by Western blot and RT-PCR are shown (Fig. 1A-C).

ASML cells have a round morphology and do not spread on plastic. These features are maintained in the ASML-CD44v^{kd} and ASML-CD44v^{rsc} clones (Fig. 1D). Besides CD44v, ASML cells express the metastasis-associated markers EpCAM, D6.1A, $\alpha_6\beta_4$, and C4.4A. Expression of these markers is unaltered in ASML-CD44v^{kd} and ASML-CD44v^{rsc} clones (Fig. 1E). The integrin expression profile was of special interest due to the importance in cell adhesion and migration. Notably, ASML^{wt} cells express several leukocyte-associated integrins. Integrin expression is also unaltered in ASML-CD44v^{kd} cells (Fig. 1F).

In summary, the knockdown of CD44v has no effect on cell morphology and no significant effect on metastasis-associated marker and adhesion molecule expression of ASML cells.

ASML-CD44v^{kd} Cells Poorly Metastasize

ASML cells hardly grow locally after intrafootpad application but readily settle in lymph nodes and the lung, where they form thousands of small tumor nodules (29). Metastasis formation of ASML^{mock} clones was unaltered compared with ASML^{wt} cells, as shown by immunohistochemical analysis of lung sections, displaying a very high tumor load (Fig. 2A and B). One of these three ASML-CD44v^{kd} clones showed enhanced local growth. All clones grew in the draining lymph nodes, but the metastatic load of the lymph nodes was significantly reduced compared with ASML^{wt} cells. Two clones did not settle in the lung and one clone formed only few miliary nodules in 3 of 6 rats. Two ASML-CD44v^{rsc} clones expressing CD44v6/v7 formed miliary metastases in the lung (5 of 6 and 6 of 6 rats), although the metastatic load was reduced compared with ASML^{wt} cells. From 12 rats receiving two ASML-CD44v^{rsc} clones expressing CD44v4-v7, all developed miliary metastases in the lung. Notably, the rescue clones were derived from one of the ASML-CD44v^{kd} clones, which were not settling in the lung (Table 1). Immunohistology of lung sections and Western blot of *ex vivo* cultured or freshly harvested lung and lymph node tissue from rats that received CD44v^{kd} or CD44v^{resc} clones revealed that knockdown and rescue clones remained stable *in vivo*. The few metastatic nodules in the lung and lymph node metastases of rats receiving clone CD44v7i-16 expressed the ASML markers C4.4A and EpCAM but not CD44v6. Instead, ASML-CD44v^{rsc} cells recovered from lung and lymph nodes expressed CD44v6/v7 or CD44v4-v7 (Fig. 2C).

Thus, CD44v6/v7 is essential for metastatic growth of ASML cells in lymph nodes and the lung, with reduced expression (ASML-CD44v^{rsc}) obviously being sufficient to restore the metastatic phenotype of ASML cells.

CD44v^{kd} Is Accompanied by a Striking Loss in Apoptosis Resistance

Cell cycle progression and apoptosis resistance have been associated with functional importance of CD44 in tumor progression (2, 3, 9). There is evidence that these activities can be connected to hyaluronan binding of CD44 (10). It is also disputed that some of these activities are strengthened by or dependent on CD44v expression (9).

ASML cells have a slow cell cycle that is not affected by the CD44v^{kd}, no matter whether cells are cultured in medium containing 0.5% FCS (data not shown) or 10% FCS (Supplementary Fig. S1). Anchorage-independent growth, another important feature in tumor progression, also is not affected in ASML-CD44v^{kd} cells. Soft agar colony-forming efficacy of ASML^{wt} and ASML-CD44v^{kd} cells was in the range of 96.4 $\pm$ 3.4% and 94.3 $\pm$ 4.1%.

However, ASML^{wt}/ASML^{mock} cells are strikingly cisplatin and γ-irradiation resistant and resistance is strongly reduced in ASML-CD44v^{kd} cells. The LD_{50} (dose to kill 50% of cells) for ASML^{wt}/ASML^{mock} is in the range of 45 μg cisplatin and >600 Gy. Drug and irradiation resistance of ASML-CD44v^{kd} cells is 3- to 5-fold decreased. Neither the CD44v4-v7^{rsc} nor the CD44v6/v7^{rsc} sufficed to restore γ-irradiation and drug resistance (Fig. 3A and B). The latter may be due to the reduced overall expression of CD44v compared with ASML^{wt} cells. Nonetheless, ASML-CD44v^{rsc} cells metastasize, which implies that apoptosis resistance is not essentially required for tumor progression. Because ASML-CD44v^{rsc} cells formed significantly fewer metastatic nodules than ASML^{wt} cells, it is likely that apoptosis resistance contributes to the efficacy of metastasis formation. Thus, we investigated the relevant metabolic pathways.

Because CD44 has been shown to interfere with apoptotic cell death via different routes, we first examined the influence of specific inhibitors. Whereas a MEK1/2 inhibitor has no effect, γ-irradiated ASML-CD44v^{kd} cells do not survive

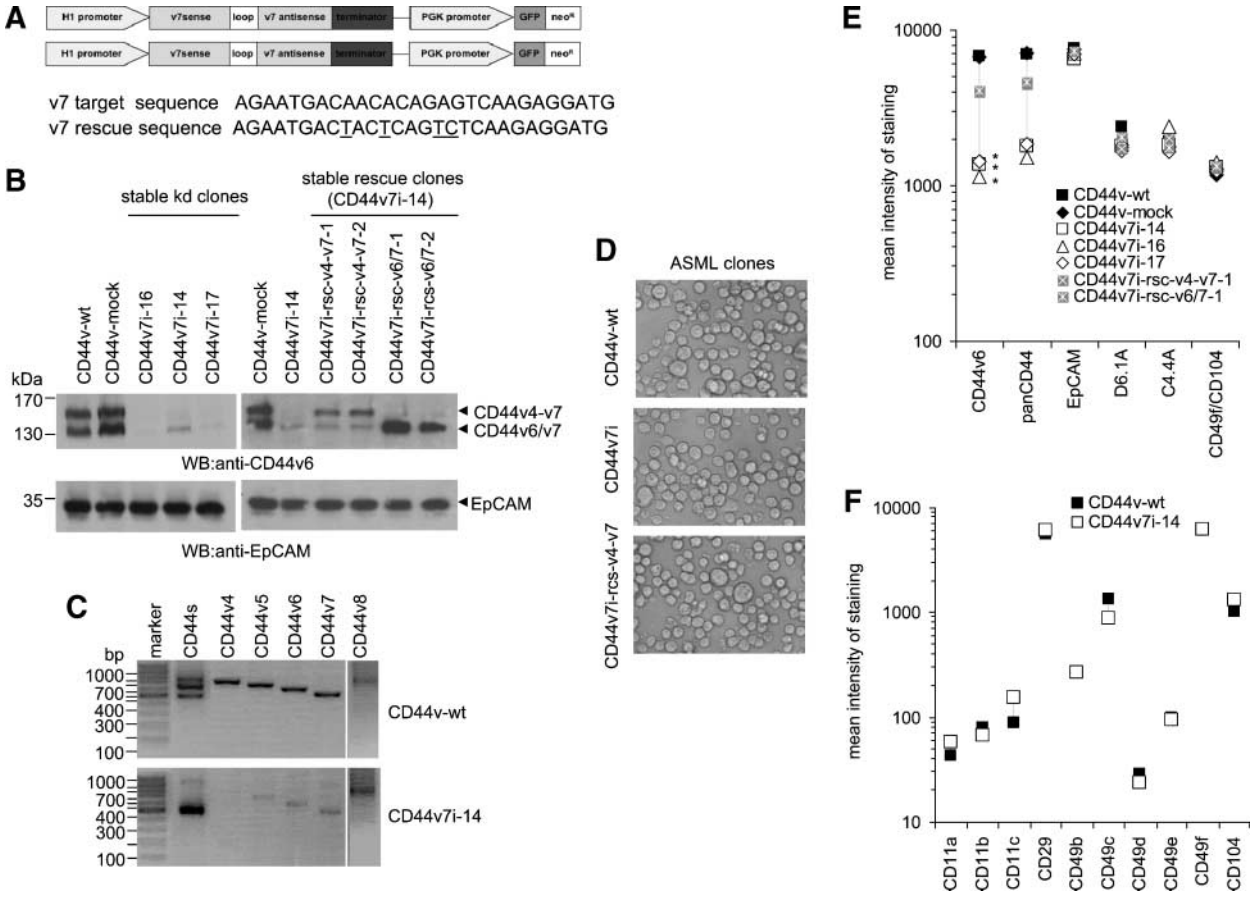

FIGURE 1. Generation of ASML-CD44v^{kd} and ASML-CD44v^{rsc} clones. **A.** Sequence of the RNAi knockdown and the RNAi rescue. **B.** Efficacy of the CD44v7 RNAi knockdown and a CD44v4-v7 or CD44v6/v7 RNAi rescue: after SDS-PAGE, lysates of ASML^{wt}, ASML^{mock} (ASML transfected with the empty vector), three ASML-CD44v^{kd}, and four ASML-CD44v^{rsc} (derived from CD44v7i-14) clones were blotted with anti-CD44v6 and anti-EpCAM (loading control). Arrow, bands corresponding to CD44v4-v7 and CD44v6/v7. ASML-CD44v^{kd} show hardly detectable levels of CD44v4-v7 or CD44v6/v7. ASML-CD44v4-v7^{rsc} and ASML-CD44v6/v7^{resc} cells express either CD44v4-v7 or CD44v6/v7. **C.** Expression of CD44 isoforms in ASML^{wt} and ASML-CD44v^{kd} clones as revealed by RT-PCR. ASML cells express CD44s (weakly), CD44v4-v7, and CD44v6/v7. They also express very weakly the CD44v8-v10 isoform. CD44s and CD44v8-v10 expression are not affected by the CD44v4-v7 knockdown. **D.** Light microscopy of ASML^{wt}, ASML-CD44v^{kd}, and ASML-CD44v^{rsc} cells, which all three grow adherent but do not spread. **E.** Flow cytometry analysis of CD44v6 and additional metastasis-associated marker expression in ASML^{wt}, ASML^{mock}, ASML-CD44v^{kd}, and ASML-CD44v^{rsc} cells. **F.** Flow cytometry analysis of integrin expression in ASML^{wt} and ASML-CD44v^{kd} cells. **E** and **F.** Mean intensity. Asterisk, significant differences. Only the mean intensity of CD44v6 expression is strongly decreased in ASML-CD44v^{kd} and partially regained in ASML-CD44v^{rsc} cells.

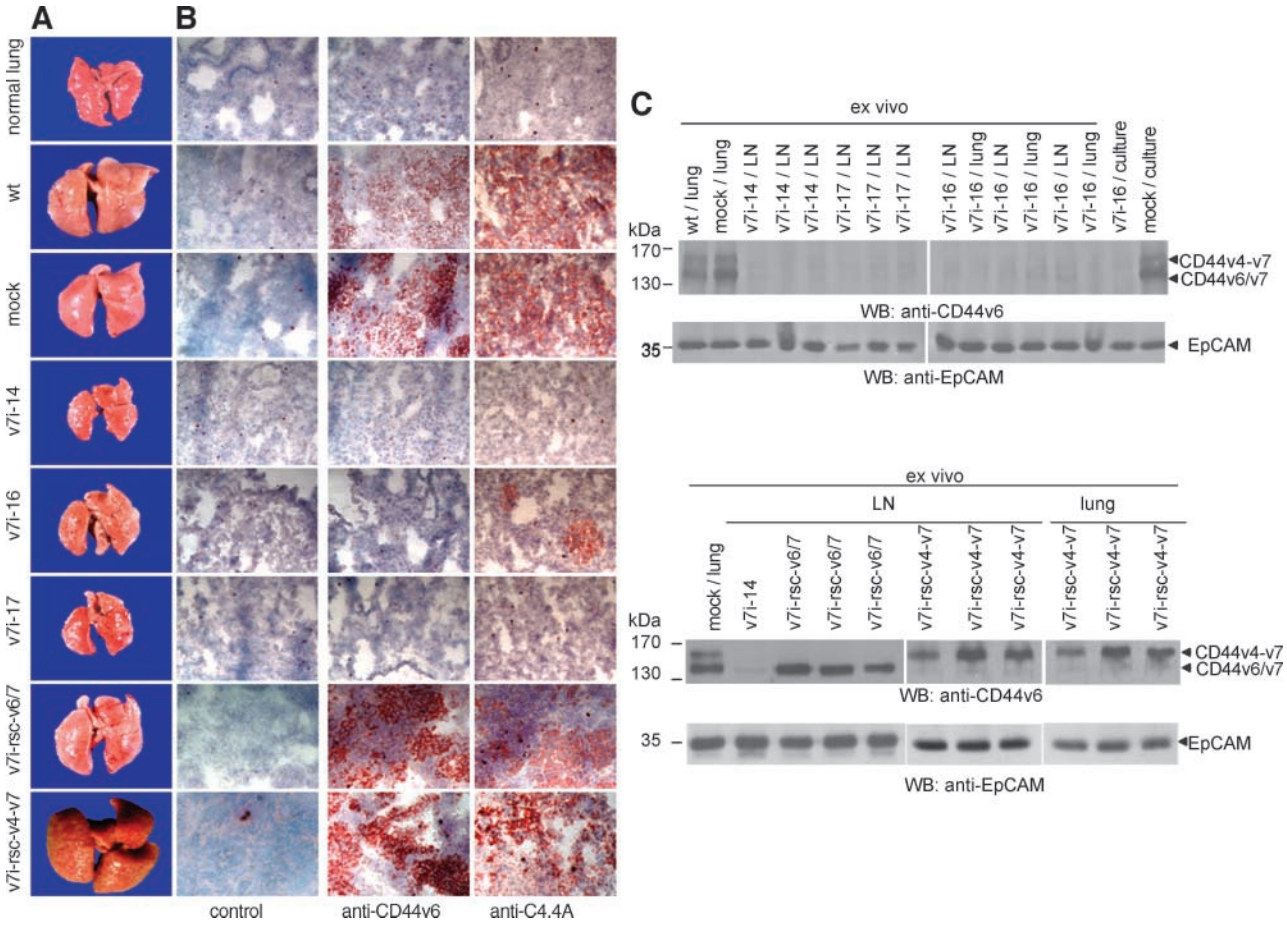

FIGURE 2. Loss of metastasis formation of ASML-CD44v^{kd} cells. Rats were sacrificed 60 d after intrafootpad injection of 1×10^6 tumor cells. **A.** Macroscopic appearance of a normal rat lung, a lung of ASML^{wt}, ASML^{mock}, three ASML-CD44v^{kd}, one ASML-CD44v6/v7^{rsc}, and one ASML-CD44v4-v7^{rsc} clones of rats. **B.** Shock frozen lung sections (5 μm) were stained with anti-CD44v6 (A2.6) and anti-C4.4A (C4.4), a metastasis marker highly expressed on ASML cells. Representative examples: abundant metastases (CD44v6$^+$, C4.4A$^+$) in the lungs of rats receiving ASML^{wt} and ASML^{mock} cells, no metastases in the lungs of ASML-CD44v^{kd} clone v7i-14 and v7i-17, few metastases in clone v7i-16 (CD44v6$^-$, identified by staining with C4.4), and abundant metastases in v7i-14rsc.v6/v7 and v7i-resc-v4-v7 (CD44v6$^+$, C4.4A$^+$). **C.** Lung and lymph nodes from rats bearing ASML^{wt}, ASML^{mock}, ASML-CD44v^{kd}, and ASML-CD44v6/v7^{rsc} tumors were dispersed and maintained in culture for 2 wk. As far as tumor cells grew, they were lysed and after SDS-PAGE, blotted with anti-CD44v6 and anti-EpCAM (loading control). Lung and lymph nodes from ASML-CD44v4-v7^{rsc}-bearing rats were meshed, directly lysed, and after SDS-PAGE, blotted as above. Each lane represents lysates from lymph nodes or the lung from a distinct rat. The last two lanes (*top*) show CD44v and EpCAM expression in the respective clones before *in vivo* passage. CD44v6 was only detected in ASML^{wt}, ASML^{mock}, and ASML-CD44v^{rsc} cultures, confirming the *in vivo* stability of the knockdown and the rescue.

50 μmol/L of the PI3K inhibitor LY294002, which also suffices for a reduction in the survival rate of γ-irradiated ASML^{wt} cells (Fig. 3C). However, without any additional apoptotic trigger, the LD_{50} of LY294002 for ASML^{wt} cells is three to four times higher than for ASML-CD44v^{kd} cells. The susceptibility of the ASML-CD44v^{rsc} clones remains in the same range as that of ASML-CD44v^{kd} clones. Similar results were obtained when Akt inhibitor II was applied (Supplementary Fig. S2A and B). In contrast, even a high dose of a MEK1/2 inhibitor did not induce cell death (data not shown). These findings suggest an involvement of the PI3K/Akt pathway.

In line with this hypothesis, expression of Bcl-2 and Bcl-xL is reduced in ASML-CD44v^{kd} compared with ASML^{wt}/ASML^{mock} cells and Bcl-2 expression becomes strongly down-regulated in cisplatin-treated (10 μg/mL) ASML-CD44v^{kd} but not ASML^{mock} cells. Whereas phosphorylation of extracellular signal-regulated kinase 1/2 (ERK1/2), one of the downstream signaling molecules in the mitogen-activated protein kinase pathway, is only slightly reduced in untreated and cisplatin-treated ASML-CD44v^{kd} compared with ASML^{wt} cells, Akt phosphorylation is significantly reduced in cisplatin-treated ASML-CD44v^{kd} but not ASML^{mock} cells (Fig. 3D). Notably, CD44v6 cross-linking in ASML^{wt} cells and cross-linking with high molecular weight hyaluronan (data not shown) promote phosphorylation of CD44-associated proteins and suffice for Akt phosphorylation (Fig. 3E). Thus, CD44v contributes to apoptosis resistance of ASML cells via up-regulated activity of the PI3K/Akt pathway.

It has been described that CD44 via its interaction with the tumor matrix contributes to apoptosis resistance. Therefore, and to strengthen this assumption on a direct involvement of CD44v in apoptosis resistance, we controlled for apoptosis resistance, when ASML cells were seeded on their own matrix. Seeding ASML^{wt} cells on their own matrix resulted in a significant

increase in apoptosis resistance. In comparison, survival of neither ASML^{wt} nor ASML-CD44v^{kd} cells was increased when seeded on the ASML-CD44v^{kd} matrix (kd-matrix). Also, apoptosis resistance of ASML-CD44v^{kd} cells was not strengthened when seeded on the ASML^{wt} matrix (wt-matrix; Fig. 3F), which confirms the direct involvement of CD44v in apoptosis resistance. The results also provide first evidence for a feedback mechanism, between ASML^{wt} cells and their matrix, which obviously provides the initiating trigger for CD44v-transduced antiapoptotic signals.

ASML^{wt} but not ASML-CD44v^{kd} Cells Generate an Adhesive Matrix

Matrix adhesion and modulation is an important factor in tumor progression (33, 34) and CD44 has been suggested to contribute to tumor progression via hyaluronan binding (10). Because apoptosis resistance of ASML^{wt} cells is supported by the tumor matrix, we proceeded to explore the matrix secreted by ASML^{wt} in comparison with the ASML-CD44v^{kd} cells. It should be noted that ASML^{wt} cells attach to plastic only after ~24 h and require 3 to 4 h for partial attachment to extracellular matrix components. On the other hand, plastic-adherent ASML^{wt} cells are very hard to detach by trypsin/EDTA (30). These findings suggest that ASML^{wt} cells may only or at least preferentially adhere to their own matrix.

In fact, the ASML^{wt} (wt) and the ASML-CD44v^{kd} (kd) matrix display striking functional differences. ASML^{wt} cells secrete an adhesive matrix, to which ASML^{wt}, ASML-CD44v^{kd}, and ASML-CD44v^{rsc} cells adhere within 5 to 10 min. All these cells hardly adhere to the kd-matrix. This adhesive feature of the wt-matrix is partly restored in the matrix of ASML-CD44v^{rsc} clones (Fig. 4A).

In a first attempt to identify possible differences between the wt-matrix and the kd-matrix, ASML cells and the deposited matrix were stained with matrix-specific antibodies. The deposited matrix contains collagen I to IV, fibronectin, hyaluronan, laminin 1, tenascin, thrombospondin, and vitronectin. Hyaluronan, laminin 1, thrombospondin, and vitronectin are most abundantly secreted. Collagens I and II were most abundant at cell matrix contact sites; collagens III and IV and laminin B2 were enriched in close proximity to the cell. Fibronectin, laminin, vitronectin, and thrombospondin were equally distributed with an enrichment in close proximity to the cell. Hyaluronan appeared to be equally distributed in a cell-independent manner, but deposited hyaluronan derived from ASML^{wt} cells seems to be more structured than hyaluronan derived from ASML-CD44v^{kd} cells. However, matrix components in the deposited matrix of ASML-CD44v^{kd} cells apparently do not significantly differ from that of ASML^{wt} cells (data not shown). Also, atomic force microscopy (AFM) did not reveal obvious differences between the two matrices (data not shown).

However, AFM confirmed the distinct functional nature of the wt-matrix versus the kd-matrix. Both ASML^{wt} and ASML-CD44v^{kd} cells spread and display, as a result, robust spike-like protrusions on the wt-matrix. This prominent feature is absent in both cell types on seeding on the kd-matrix. Instead, these cells display a rounded morphology and are highly motile during scanning (Fig. 4B and C).

CD44 is known to be involved in the assembly of pericellular matrices through anchoring hyaluronan (10). However, neither were ASML cells coated with a pericellular matrix as revealed by particle exclusion assays (data not shown) nor was the adhesive fraction of the matrix associated with membrane material as shown by 100,000 × *g* centrifugation. Only the soluble fraction, which contains shed CD44, supported cell adhesion (Supplementary Fig. S3A). By size chromatography, Superdex200 (void volume; data not shown), and CL6B Sepharose (fractions 20-22), adhesiveness was confined to a factor/complex with a putative molecular weight between 600 and 4,000 kDa (Supplementary Fig. S3B). SDS-PAGE separation of the adhesive fractions of the wt-matrix and kd-matrix revealed differences in the high molecular weight band patterns, with at least one band appearing weaker in the kd-matrix (Supplementary Fig. S3C, *arrow*). Thus far, lamininB2 was identified by mass spectrometry as one potential

Table 1. Strong Reduction in Metastatic Progression of ASML-CD44v^{kd} Clones

Tumor	Tumor take	Lymph node metastasis			Lung metastasis				
		Incidence	Weight (g)*	*P*	Incidence	No. miliary metastasis †	*P* ‡	Weight (g)	*P* ‡
None	—	—	—		—	—		1.3 ± 0.1	
ASML^{wt}	6/6	6/6	6.9 ± 1.7		6/6	>5,000		5.1 ± 0.7	
ASML^{mock}	12/12	12/12	6.9 ± 1.4	NS	12/12	>5,000	NS	5.6 ± 0.8	
ASML-CD44v7i-16	6/6	6/6	4.5 ± 1.2	0.017	3/6	0, 0, 0, 3, 7, 52	<0.0001	1.8 ± 0.7	<0.0001
ASML-CD44v7i-17	6/6	6/6	2.3 ± 0.9	<0.0001	0/6	0	<0.0001	1.4 ± 0.1	<0.0001
ASML-CD44v7i-14	12/12	12/12	3.3 ± 0.7	<0.0001	0/12	0	<0.0001	1.3 ± 0.2	<0.0001
ASML-CD44v7i-14 rsc.v6/v7-1	6/6	6/6	6.2 ± 1.3	NS **0.0085**	5/6	0, 9, 159, 178, >5,000, >5,000	0.0003 **0.0283**	2.9 ± 1.2	0.0026 **0.0096**
ASML-CD44v7i-14 rsc.v6/v7-2	6/6	6/6	7.2 ± 2.7	NS **0.0070**	6/6	150, 200, 230, 300, 350, 600	<0.0001 **0.0009**	2.5 ± 0.4	<0.0001 **0.0402**
ASML-CD44v7i-14 rsc.v4-v7-1	6/6	6/6	7.0 ± 1.6	NS **0.0004**	6/6	175, 500, 500, 1,000, >5,000, >5,000	0.0105 **0.0505**	3.9 ± 1.3	NS **0.0042**
ASML-CD44v7i-14 rsc.v4-v7-2	6/6	6/6	7.9 ± 1.9	NS **0.0002**	6/6	750, 5× >5,000	NS **0.0031**	5.6 ± 1.2	NS **0.0001**

*Estimate according to the volume of the pooled metastatic lymph nodes.
† Lung surface visible metastatic nodules; >5,000: confluent.
‡ *P* values: in comparison with ASML^{wt}, bold *P* values: ASML-CD44v7i-14-rsc.v6/v7 and ASML-CD44v7i-14-rsc.v4-v7 in comparison with ASML-CD44v7i-14.

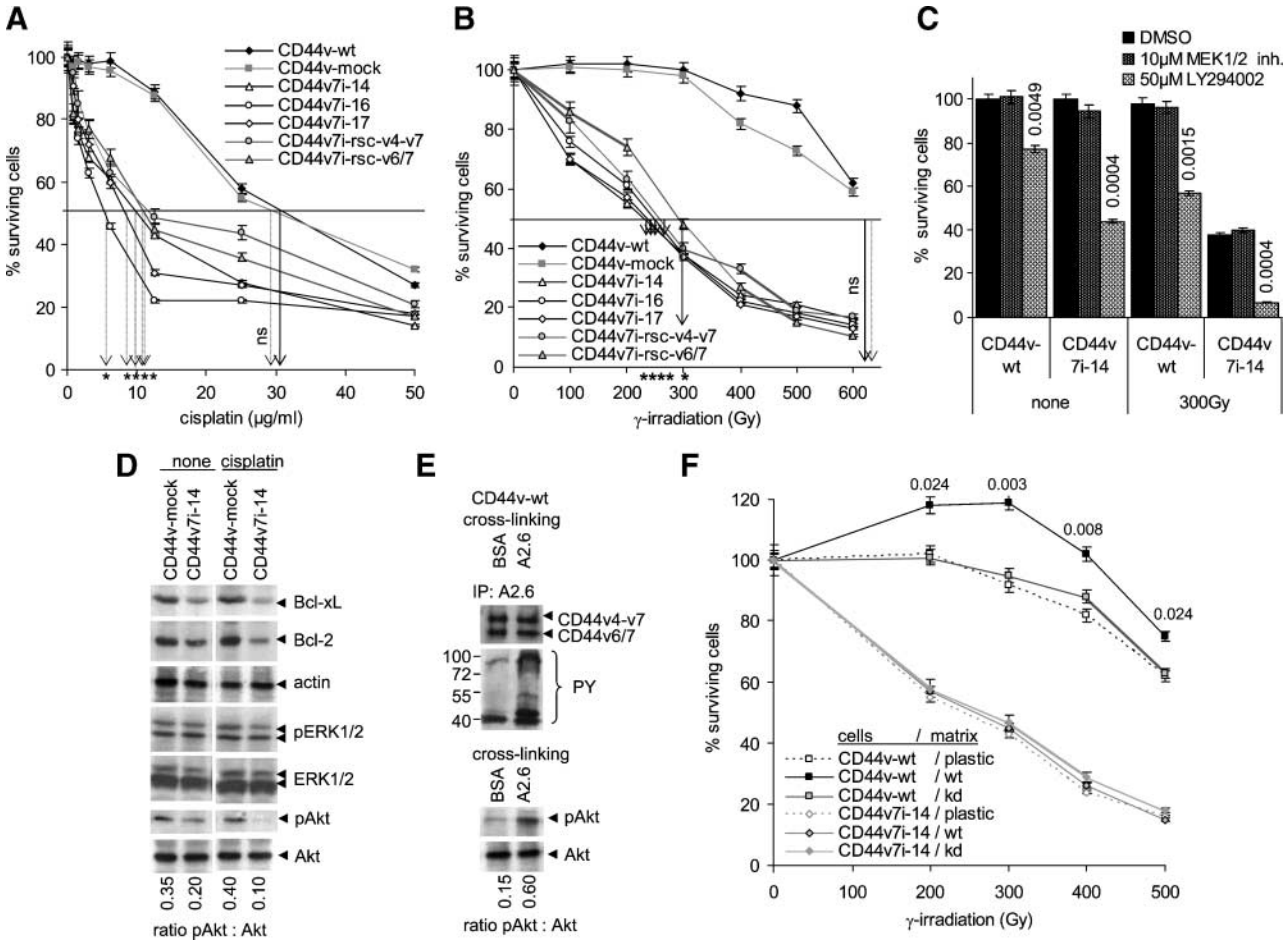

FIGURE 3. Apoptosis resistance and PI3K/Akt signaling in ASML^{wt} and ASML-CD44v^{kd} cells. **A** and **B.** ASML^{wt}, ASML^{mock}, ASML-CD44v^{kd}, and ASML-CD44v^{rsc} cells were seeded on plastic. After 24 h, (**A**) cisplatin was added at the indicated concentrations or (**B**) cells were irradiated. Survival was estimated by MTT uptake after 3 d. Mean ± SD of triplicates compared with untreated cells (100%). *, $P < 0.01$, significant differences in the dose of cisplatin or irradiation required for 50% reduction in MTT uptake. **C.** ASML^{wt} and ASML-CD44v^{kd} cells were nonirradiated or irradiated with 300 Gy and cultured in the presence of 50 μmol/L LY294002 (PI3K inhibitor) or 10 μmol/L MEK1/2 inhibitor. The percentage of surviving cells was evaluated after 72 h (MTT assay; survival of untreated cells = 100%). **D.** ASML^{wt} and ASML-CD44v^{kd} cells were treated with cisplatin (10 μg/mL). Untreated and cisplatin-treated cells were lysed after 24 h. After SDS-PAGE, lysates were blotted with anti-Bcl-2, anti-Bcl-xL, anti-actin (loading control), anti-pERK1/2, and anti-ERK1/2 (loading control) or anti-pAkt and anti-Akt (loading control). **E.** ASML^{wt} cells were biotinylated and seeded on bovine serum albumin or anti-CD44v6 (A2.6)-coated plates (2 h). Lysates were either immunoprecipitated with anti-CD44v6 or directly subjected to SDS-PAGE. Membranes were blotted with streptavidin for the detection of precipitated CD44v and with anti-phosphotyrosine or were blotted with anti-pAkt and anti-Akt (loading control). CD44v cross-linking induced PTK and Akt activation. **F.** ASML and ASML-CD44v^{kd} cells were seeded on plastic or wt-matrix or kd-matrix. After 24 h, cells were irradiated. Survival was estimated by MTT uptake after 3 d. Mean ± SD of triplicates compared with untreated cells (100%). Asterisk, significant differences in MTT uptake compared with cells seeded on plastic.

candidate. Western blot of the adhesive fraction of the wt-matrix, which does not contain shed CD44v, confirmed the presence of laminins. However, laminins are also found in the corresponding fractions of the kd-matrix (Supplementary Fig. S3D).

We proceeded to search for a potential, specific ligand-receptor interaction. As CD44v^{kd} cells do not display impaired adhesion to the wt-matrix, adhesion is not mediated by CD44v. Accordingly, adhesion could not be blocked by anti-CD44v6 or anti-panCD44. Instead, anti-integrin β_1 strongly interferes with cell adhesion, whereas blocking anti-α_3 and anti-α_2 antibodies had no such effect (Fig. 5A). Thus, cells adhere to the matrix via a β_1 integrin. An anti-laminin antibody does not block ASML^{wt} cell adhesion. In contrast, collagenase treatment destroys the adhesive properties of the matrix, arguing for a collagen-mediated adhesion, where the collagen type remains to be identified (Fig. 5B).

Because CD44 itself is apparently not involved in the adhesion process to the wt-matrix, the question arose why ASML-CD44v^{kd} cells do not assemble an adhesive matrix. CD44v seems to contribute to matrix production via an interaction with hyaluronan. Hyaluronidase treatment of a coated matrix does not interfere with adhesion, whereas treatment before coating destroys the adhesive feature. This argues for hyaluronan serving as a scaffold for other matrix components and implies an essential involvement of CD44v during assembly (Fig. 5C).

In summary, only ASML^{wt} cells produce a collagen-containing matrix, which facilitates rapid adhesion of ASML^{wt} and ASML-CD44v^{kd} cells via a β_1 integrin. This

feature is essentially absent in a kd-matrix, although ASML-CD44v^{kd} cells adhere and spread on the wt-matrix. Thus, CD44v is essential for the production of this adhesive matrix but not for the adhesion. CD44v also facilitates apoptosis resistance in ASML cells. Reduced CD44v6/v7 expression (ASML-CD44v^{rsc}) does not support survival but suffices to promote matrix assembly and metastatic spread. Thus, the involvement of CD44v in matrix assembly is essential for settlement and growth in the lung.

Discussion

Only few cells within a tumor are tumorigenic and possess the capacity to metastasize (6). Recently, signatures of these CIC have been identified for several tumor types (35) and CD44 is one of these CIC markers shared by different tumor types including pancreatic adenocarcinoma (36), which emphasizes its role in metastasis promotion. However, little is known about pathways, whereby these CIC markers contribute to tumor progression. We here addressed the mechanism of tumor progression for the CD44v4-v7 isoform in the well-characterized ASML tumor model by a selective knockdown. Indeed, CD44v6/v7 expression is essential for metastasis formation of these cells without affecting proliferation or colony-forming efficacy. The capacity of ASML-CD44v^{kd} cells to settle and grow in lymph nodes is strongly reduced and they hardly settle and grow in the lung, which is reversed again in CD44v6/v7 and CD44v4-v7 rescue clones. We propose that at least two superimposing functions of CD44v allow these cells to metastasize: adhesiveness is the decisive feature and apoptosis resistance accounts for the efficacy of individual cells to form a metastasis.

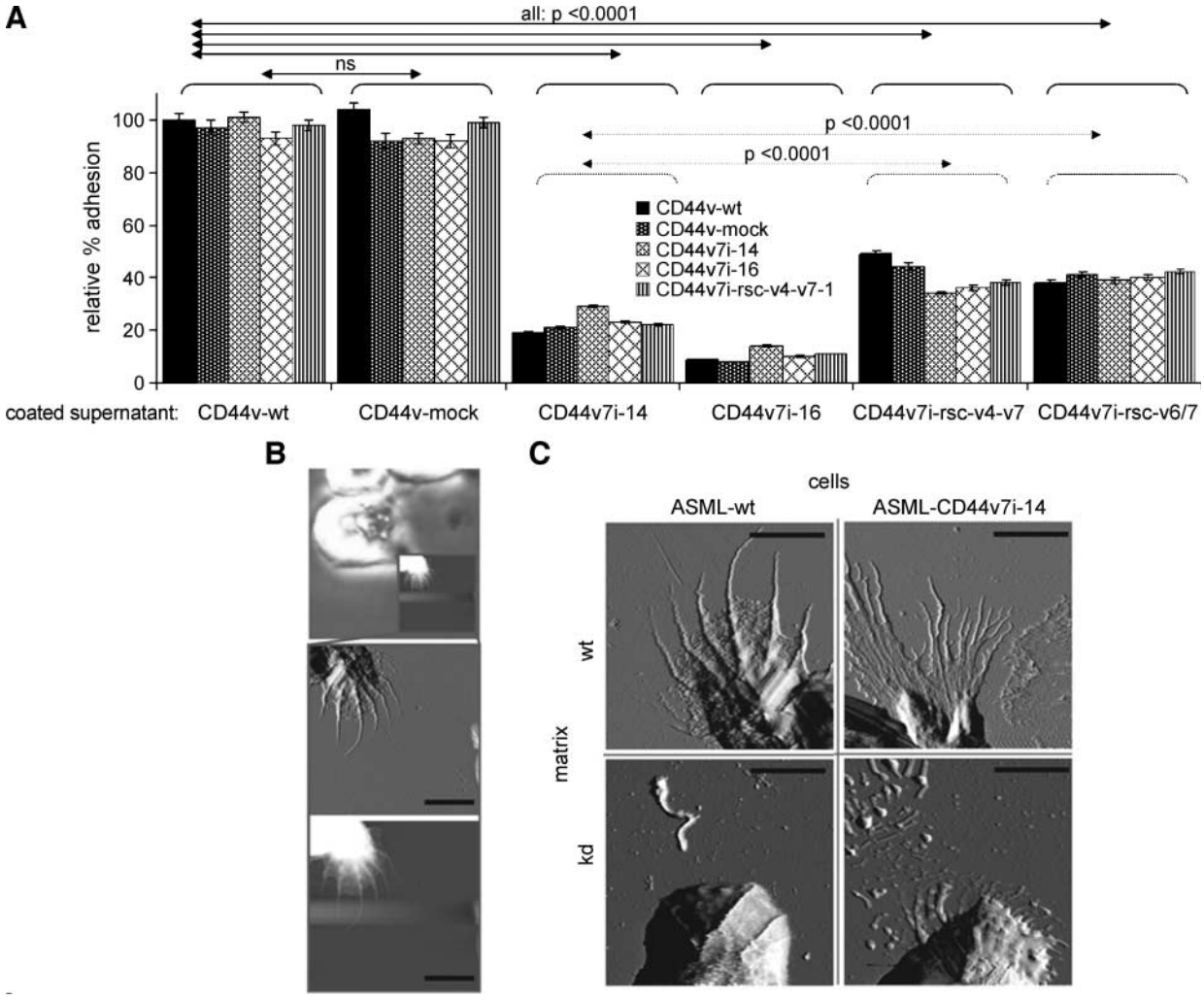

FIGURE 4. ASML cells secrete an adhesive matrix. **A.** ASML^{wt}/ASML^{mock}, ASML-CD44v^{kd}, and ASML-CD44v^{rsc} cells were seeded in 24-well plates coated with ASML^{wt}/ASML^{mock}, ASML-CD44v^{kd}, and ASML-CD44v^{rsc} cell culture supernatant and incubated for 10 min. After washing, adherent cells were stained with crystal violet and lysed. Absorption was determined at 595 nm. Mean ± SD of triplicates compared with adhesion of ASML^{wt} cells to the wt-matrix (100%; corresponds to ~30% of total ASML^{wt} cells; <1% adhere to plastic within 10 min). Although ASML^{wt}/ASML^{mock}, ASML-CD44v^{kd}, and ASML-CD44v^{rsc} cells adhere with comparable efficacy to the different matrices, their adhesion to the kd-matrix is significantly reduced; adhesion to the rsc- compared with the kd-matrix is significantly increased. **B** and **C.** Morphometric imaging of ASML cells on distinct matrices by AFM. **B.** Representative AFM image of an ASML^{wt} cells 24 h after seeding on wt-matrix; from top to bottom, direct overlay of the optical and AFM image, height image, with a color scale corresponding to 840 nm and "error image" derived from the cantilever deflection signal. **C.** Representative AFM images of ASML^{wt} and ASML-CD44v^{kd} cells on wt-matrix and kd-matrix. Bar, 5 μm.

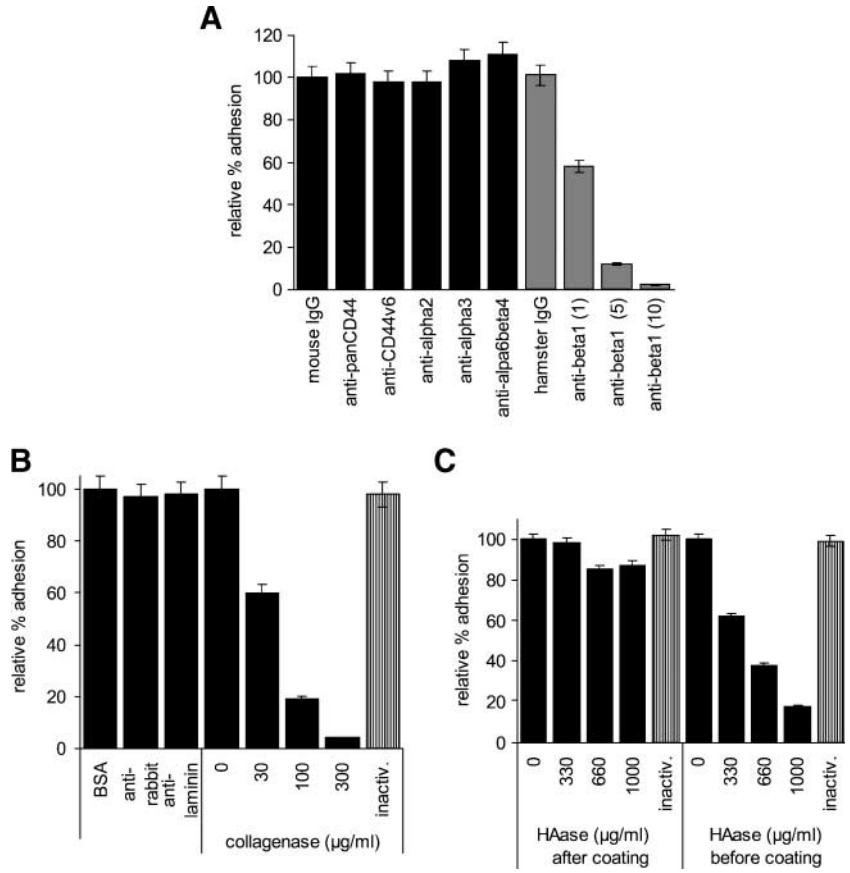

FIGURE 5. Assembly of the wt-matrix and integrin-mediated adhesion. **A.** ASML^{wt} cells were incubated with the indicated antibodies including the respective isotype controls (10 μg/mL or, where indicated, 1-10 μg/mL; 30 min, 4°C), washed, and seeded in 24-well plates coated with ASML^{wt} supernatant. Anti-β_1 but not anti-CD44s or anti-CD44v6 blocked ASML cell adhesion. **B.** 24-well plates were coated with ASML^{wt} supernatant. Coated plates were treated with bovine serum albumin, control IgG, or a polyclonal anti-laminin antibody (10 μg/mL) or an increasing dose of collagenase including heat-inactivated (95°C, 20 min) collagenase as a negative control. Adhesion of ASML^{wt} cells was not prevented by blockade of laminin, but ASML^{wt} cells did not adhere to collagenase-treated coated matrix. **C.** 24-well plates were coated with ASML^{wt} supernatant and coated plates were treated with hyaluronidase or ASML^{wt} supernatant was treated with an increasing dose of hyaluronidase and was coated thereafter on 24-well plates. Heat-inactivated hyaluronidase (95°C, 20 min) served as a negative control. Hyaluronidase did not destroy adhesiveness of the coated matrix. Instead, treatment of the conditioned supernatant with hyaluronidase interfered with ASML^{wt} cell adhesion. **A** to **C.** Mean ± SD of triplicates (crystal violet staining) compared with ASML^{wt} cell adhesion to the wt-matrix (100%).

CD44v and Apoptosis Protection

Apoptosis at the metastatic site is thought to be a limiting step after the spread of tumor cells (37). The high apoptosis resistance of ASML^{wt} cells (30) is severely impaired in ASML-CD44v^{kd} cells. We did not find CD44-related differences in multidrug resistance and death receptor-mediated apoptosis (data not shown). Mitogen-activated protein kinase signaling also does not seem to play a central role. Instead and in line with several reports (28, 38), activation of the PI3K/Akt pathway obviously is decisive. CD44v cross-linking promotes Akt phosphorylation in ASML^{wt} cells; accordingly, ASML-CD44v^{kd} cells display impaired PI3K/Akt signaling.

CD44v is likely to be involved directly in apoptosis resistance, because this feature cannot be imparted to ASML-CD44v^{kd} cells by the wt-matrix, although these cells adhere to the wt-matrix via β_1 integrins. Thus, CD44 cross-linking via matrix components may well be the initial trigger for activation of antiapoptotic molecules (10), which proceeds via CD44v6. Activation of PI3K via CD44 has repeatedly been reported (39-41). Although we did not observe a direct association between CD44 and PI3K, this does not exclude PI3K activation by downstream signals of CD44. Signals possibly could be transmitted through CD44-associated integrins (42), which can be activated via CD44v ligand binding (27). In fact, CD44 is associated with α_3 and β_1 integrin chains in ASML^{wt} cells, but cross-linking of α_3 or β_1 does not promote PI3K/Akt activation (data not shown). We hypothesize that CD44 engagement in ASML cells triggers a CD44-PTK association and PTK activation. Such associations have repeatedly been shown for CD44/CD44v (39, 40, 43, 44) and could be shown for ASML^{wt} but not ASML-CD44v^{rsc} cells. We noted an increased association between CD44v6 and c-Src in ASML cells, which was accompanied by increased activation of the focal adhesion kinase,[5] which can trigger PI3K activation. It also has been described that c-met supports tumor cell survival via PI3K/Akt activation (45, 46) and that c-met interacts with CD44v6 via hepatocyte growth factor/scatter factor binding (23). Notably, c-met activity is significantly reduced in ASML-CD44v^{kd} cells.[5] Taken together, the ASML matrix (see below) might act as a reservoir for growth factors such as hepatocyte growth factor/scatter factor (47). Concomitantly, appropriately assembled hyaluronan could act as the initial trigger leading to CD44 clustering. This can be accompanied by relocation of CD44 to specialized membrane microdomains, which serve as signaling platforms (48, 49). Work is in progress to evaluate whether CD44v6-initiated apoptosis resistance, indeed, proceeds via assembled hyaluronan (see below) as the initial trigger, which allows CD44v6 to associate with c-Src promoting focal adhesion kinase activation and/or to recruit hepatocyte growth factor/scatter factor for c-Met activation or whether c-Met activation proceeds via activated focal adhesion kinase (50).

Restoring CD44v expression in ASML-CD44v^{kd} clones suffices to rescue the metastatic potential but not apoptosis

[5] T. Jung, unpublished finding.

resistance. There is no evidence for the expression of additional CD44v7-containing isoforms that would not have been restored. Also, CD44v4-v7 and CD44v6/v7 are the dominant isoforms (1). It may be that both isoforms are required. We consider it most likely that the overall expression level in the rescue clones might have been too low to promote Akt phosphorylation. Notably, the metastasizing AS-14 cells (1), which express CD44v4-v7 at a comparable level with ASML-CD44v^{rsc} clones, show high apoptosis susceptibility in the range of locally growing AS cells (data not shown). Thus, apoptosis resistance, although obviously affecting the efficacy of metastasis formation, may not directly contribute to the process itself. Instead, the CD44v cross-talk with the environment is decisive for proceeding through the metastatic cascade.

ASML Cells Secrete a Strongly Adhesive Matrix, Which Supports Apoptosis Resistance

ASML cells poorly adhere to plastic or individual components of the extracellular matrix but secrete a strongly adhesive matrix. Matrix production requires CD44v expression, but adhesion proceeds via β_1 integrin binding to collagen as revealed by antibody inhibition and collagenase treatment that destroys matrix adhesiveness. ASML-CD44v^{kd} cells can adhere to the wt-matrix, because their integrin expression is unaltered and CD44 is not involved in the adhesion.

Even not being the ligand, CD44v is essential for proper matrix production, which was confirmed by the partial regain of adhesiveness of the ASML-CD44v^{rsc}-derived matrix. Although according to matrix-assisted laser desorption/ionization-time of flight analysis laminin B2 is enriched in the wt-matrix (data not shown), we did not yet succeed in defining components selectively present in the wt-matrix. However, it is possible that the same components might just be assembled differently. In line with this interpretation, hyaluronan appears to be differently organized in the wt- compared with the kd-matrix. Furthermore, hyaluronidase treatment destroys matrix assembly but does not interfere with the adhesiveness of the assembled matrix, arguing for a role of CD44v and hyaluronan during proper assembly. CD44 is not present in the adhesive fractions of the matrix, which rules out a contribution to matrix formation by CD44 shedding. One could also speculate that endogenous hyaluronidase activity differs in dependence on CD44v expression or that hyaluronidase inhibitors or other matrix components protect the deposited hyaluronan (51, 52). The requirement of CD44 for pericellular matrix assembly in chondrocytes has been suggested to proceed through hyaluronan anchoring (53, 54). Yet, as outlined in these overviews, a better understanding of the hyaluronan metabolism is required to further elucidate the function of CD44v in tumor matrix assembly (53, 54).

Although the molecular and structural difference between wt-matrix and kd-matrix could not be resolved thus far, by using AFM, a fundamental functional alteration is illustrated by the appearance of adhesive cells on the different matrices. ASML^{wt} and ASML-CD44v^{kd} cells display long spikes on the wt-matrix, whereas both lines form atrophic cell protrusions on the kd-matrix. Thus, CD44v is essentially required for the secretion or the assembly or both secretion and assembly of an adhesive matrix. As revealed by the strikingly reduced metastatic potential of ASML-CD44v^{kd} cells, which cannot secrete or assemble a corresponding matrix, this matrix may well enable ASML^{wt} cells to settle and survive at secondary sites.

In conclusion, the capacity to metastasize is largely lost by a selective knockdown of CD44v in highly metastatic ASML cells. At least two features of CD44v coordinately contribute to the striking knockdown effect: CD44v is required for preparing an adhesive matrix that supports integrin-mediated adhesion and provides a trigger for apoptosis protection; ASML cells activate the PI3K/Akt survival pathway via CD44v ligand binding. Restoring the adhesive functions of CD44v suffices for lung metastasis formation. Thus, organizing the microenvironment to create a favoring surrounding for embedding and survival is the decisive feature of CD44v for initiating metastatic settlement and growth of ASML cells. CD44v interactions with the environment to receive survival-promoting signals strengthen the efficacy of metastasis formation. We propose that these complex interactions of CD44 with the microenvironment contribute to its function as a CIC marker to promote adhesion of isolated tumor cells in metastatic organs.

Materials and Methods

Rats and Tumors

BDX rats, bred at the animal facilities of the German Cancer Research Center, were kept under specific pathogen-free conditions and fed sterilized food and water *ad libitum*. ASML cells, the highly metastatic subline of a pancreatic adenocarcinoma of the BDX rat strain (24), were maintained in RPMI 1640/10% FCS (RPMI-s). Confluent cultures were trypsinized and split.

RNAi Construct and Establishment of Stable CD44v^{kd} and CD44v^{rsc} Clones

Stable CD44v^{kd} clones were generated using the pSuperGFP-neo plasmid. From three different constructs, the construct targeting exon v7 efficiently down-regulated the two most abundantly expressed CD44 isoforms (CD44v4-v7 and CD44v6/v7) in ASML cells. The construct consists of a self-complementary sequence stretch of the 28-bp target sequence and the corresponding reverse complement, separated by a 10-bp loop sequence and followed by a stretch of 5 T residues leading to termination of the transcription. Sense and antisense oligos were designed to elicit sticky ends on annealing. Oligo sequences for the v7 construct are v7 sense 5′-TCGAGAGAATGACAACACAGAGTCAAGAG-GATGCTTCCTGTCACATCCTCTTGACTCTGTGTTGT-CATTCTTTTTT-3′ and v7 antisense 5′-CTAGAAAAAAGAA-TGACAACACAGAGTCAAGAGGATGTGACAGGAAG-CATCCTCTTGACTCTGTGTTGTCATTCTC-3′. Because oligos were initially designed for *Xho*I-*Xba*I cloning, the ds insert was partially filled up and ligated into the as well partially filled up *Bgl*II/*Hin*dIII sites of the pSuper plasmid. Positive clones were verified by sequencing and used for transfections. "Rescue" clones were generated by introduction of cDNAs of either CD44v4-v7 or CD44v6/v7, in which four silent point mutations in the v7 target sequence were introduced by PCR to protect them from degradation. The knockdown clone ASML-CD44v7i1-14 was transfected with the "rescue" constructs. Stable knockdown and rescue clones were established by two rounds of recloning in selection medium.

RT-PCR

For evaluation of the presence of CD44 isoforms in ASML cells, nested RT-PCR was done using a template from 5′ primer CGACCTTTTCCAGAGGCGACTA and 3′ primer CGTCTCCAATCGTGCTGTCTTTTC. For the nested RT-PCR, the following primers were used: reverse primer (for all exons) GGCACTACCCCAATCTTC, CD44s (including all variant exons) forward primer AGACATCGATGCCTCAAAC, exon v4 forward primer TGCAACTACTCCATGGGTTT, v5 forward primer TATAGACAGAAACAGCACCA, v6 forward primer TGGGCAGATCCTAATAGCAC, v7 forward primer CTGCCTCAGCCCACAACAAC, and v8 forward primer CCAGTCATAGTACAACCCTT (32). The optimal annealing temperature was 54°C for CD44s, CD44v4, and CD44v6, 51.5°C for CD44v5, 58°C for CD44v7, and 56.9°C for CD44v8. Amplification was done for 30 cycles starting with 1 μg cDNA.

Antibodies

A2.6 (anti-CD44v6), D5.7 (anti-EpCAM), C4.4 (anti-C4.4A), D6.1 (anti-D6.1A), B5.5 (anti-$\alpha_6\beta_4$; ref. 31), Ox50 (anti-panCD44), anti-CD11b (European Association of Animal Cell Cultures), anti-thrombospondin, anti-CD11a, anti-CD11c, anti-CD29, anti-CD49b, anti-CD49c, anti-CD49d, anti-CD49e, anti-CD49f, anti-CD104, anti-laminin, anti-hyaluronan, anti-collagen I to IV, anti-fibronectin, anti-vitronectin, anti-tenascin, anti-Bcl-2, anti-Bcl-xL, anti-phosphotyrosine, anti-ERK1/2, anti-pERK1/2, anti-Akt, anti-pAkt, and streptavidin-horseradish peroxidase and dye-labeled secondary antibodies (BD/Pharmingen, Dianova, Biotrend, and Santa Cruz Biotechnology).

Flow Cytometry

Flow cytometry followed routine procedures. Samples were processed in a FACSCalibur using the Cell Quest program for analysis (BD).

Histology

Cryostat sections (5 μm) of snap-frozen lung were fixed, stained with A2.6, C4.4, or normal mouse IgG (negative control), washed, and exposed to the biotinylated secondary antibodies and alkaline phosphatase-conjugated avidin-biotin complex solution. Sections were counterstained with Mayer's hematoxylin. For fluorescence staining, cells were grown on glass coverslips, fixed, washed, and blocked (0.2% gelatin, 0.5% bovine serum albumin in PBS). For staining of deposited matrix, cells were grown for 48 h on coverslips. Cells were removed by prolonged treatment with EDTA. Slips were blocked and stained with the indicated antibodies, washed, and mounted in Elvanol. Digitized images were generated using a Leica DMRBE microscope.

Apoptosis Induction

Cells (1×10^5) cultured overnight in flat-bottomed 96-well plates were grown for 3 days in RPMI-s containing serial dilutions of cisplatin [*cis*-diamineplatinum(II) dichloride; Sigma], starting with 50 μg/mL. Alternatively, 1×10^6 cells were seeded in 35 mm Petri dishes and grown for 24 h in RPMI-s before irradiation (100-600 Gy). Survival was monitored after 72 h. Where indicated, LY294002 (PI3K inhibitor) or Akt inhibitor II or MEK1/2 inhibitor (Calbiochem) was added. The percentage of respiratory active cells was evaluated by MTT staining.

Adhesion Assay

Cells (1×10^6) were suspended in RPMI-s and seeded on plastic or different matrices in 24-well plates. Culture supernatant or the seeded matrix was treated with hyaluronidase type IV-S (330-1,000 μg/mL; Sigma) or collagenase type 2 (30-1,000 μg/mL; PAA; 2 h, 37°C). Where indicated, cells were preloaded with antibody (1-10 μg/mL; 30 min, 4°C). After incubation (10-15 min, 37°C), nonadherent cells were removed by vigorous washing. Adherent cells were fixed, stained with crystal violet, and dissolved in 10% acetic acid. Absorbance was measured at 595 nm.

Soft Agar Assay

Tumor cells were suspended in 0.5% agar and seeded on a preformed 3% agar layer. Colonies were counted at an inverted microscope after 3 weeks.

Surface Biotinylation, Lysis, and Immunoprecipitation

Cells were washed in HEPES [25 mmol/L HEPES (pH 7.2), 150 mmol/L NaCl, 5 mmol/L $MgCl_2$, 0.05% NaN_3] and incubated (30 min, 4°C) in 5 mL HEPES/0.2 mg/mL water-soluble sulfo-NHS-biotin (Calbiochem). Cells were washed in PBS/200 mmol/L glycine, resuspended in RPMI 1640, and used for activation. Cells were lysed (30 min, 4°C) in HEPES, 1% CHAPS, 1 mmol/L phenylmethylsulfonyl fluoride, 1 mmol/L $NaVO_4$, 10 mmol/L NaF, and a protease inhibitor mix (Boehringer-Mannheim). Centrifuged (13,000 × *g*; 10 min, 4°C) lysates were mixed with Laemmli buffer [62.5 mmol/L Tris-HCl (pH 6.8), 2% SDS, 25% glycerol, 0.01% bromophenol blue] and resolved by SDS-PAGE or immunoprecipitated (1 h, 4°C) followed by incubation with protein G Sepharose (1 h). Immune complexes were washed four times with lysis buffer, dissolved in Laemmli buffer, and resolved by SDS-PAGE.

SDS-PAGE and Western Blot

Samples were resolved on 6% SDS-PAGE and silver stained or resolved on 8% to 12% SDS-PAGE and proteins were transferred to nitrocellulose membrane (Amersham; 30 V; 16 h, 4°C). Membranes were blocked (PBS/0.5% bovine serum albumin/0.1% Tween 20; 1 h, room temperature) and blotted with streptavidin or primary antibodies followed by horseradish peroxidase-conjugated secondary antibodies (1 h, room temperature). Blots were developed with the ECL detection system.

Tumor Matrix Fractionation

Tumor cell conditioned medium (24 h, serum-free RPMI 1640) was harvested and centrifuged (800 and 1,500 × *g*; 20 min, 4°C). Vesicular material was sedimented (100,000 × *g*; 10 h). Supernatants were concentrated and passaged over Superdex200 or CL6B columns. Fractions were coated to evaluate adhesion or precipitated for SDS-PAGE.

Atomic Force Microscopy

In brief, AFM is based on the linewise scanning of surfaces with a thin silicon probe to generate morphometric, three-dimensional topographies of surfaces at a nanometer scale. $ASML^{wt}$ and $ASML^{kd}$ cells were seeded on round, 22 mm glass coverslips to secrete and deposit their individual matrices. Cells were detached 24 h after seeding by EDTA treatment. Detached cells were then reseeded either on their own matrix (wt-cells on wt-matrix and kd-cells on kd-matrix) or on a distinct matrix (wt-cells on kd-matrix and kd-cells on wt-matrix). After 24 h, these cells were fixed for 15 min at room temperature with glutaraldehyde at a final concentration of 0.5% in PBS (containing calcium and magnesium) and stored at 4°C in PBS/0.1% glutaraldehyde. Imaging was done with a Nano-Wizard II (JPK-Instruments) AFM mounted on an inverted microscope (Axiovert 200; Zeiss) in PBS at room temperature. Samples were scanned in contact mode with DNP tips (spring constant 0.06 N/m; Veeco) at a scan rate of 0.3 Hz. Calibration of optical images was done with the software routines built into the AFM control software before scanning the samples (DirectOverlay; JPK-Instruments). This function allows the direct correlation of optical images with real-space AFM images. Image analysis was done with the software supplied with the instrument (IP; JKP-Instruments).

In vivo *Metastasis Assay*

$ASML^{wt}$, $ASML^{mock}$, ASML-$CD44v^{kd}$, and ASML-$CD44v^{rsc}$ (rescue) cells (1×10^6) were suspended in 25 μL PBS and injected intrafootpad in 10- to 14-week-old female BDX rats. Local tumor growth and growth in draining lymph nodes were controlled weekly. All animals in one experimental setting were sacrificed simultaneously after 8 weeks or latest when the draining lymph node reached a mean diameter of 2 cm. At autopsy, the mean diameter of the local tumor and all lymph nodes was evaluated. Lungs were excised and weighed. Shock frozen sections of the lung were subjected to immunohistology staining. Lung-derived and lymph node-derived tumor cells were analyzed by Western blot for CD44v expression. Macroscopically tumor-free lymph nodes and lungs were meshed through fine gauze and seeded in culture flasks. Animal experiments were approved by the local governmental authorities.

Statistics

Significance was calculated by the Student's *t* test. Functional *in vitro* assays were repeated at least three times. Mean values are based on triplicates.

Disclosure of Potential Conflicts of Interest

No potential conflicts of interest were disclosed.

References

1. Günthert U, Hofmann M, Rudy W, et al. A new variant of glycoprotein CD44 confers metastatic potential to rat carcinoma cells. Cell 1991;65:13–24.

2. Naor D, Sionov RV, Ish-Shalom D. CD44: structure, function, and association with the malignant process. Adv Cancer Res 1997;71:241–319.

3. Marhaba R, Zöller M. CD44 in cancer progression: adhesion, migration and growth regulation. J Mol Histol 2004;35:211–31.

4. Sales KM, Winslet MC, Seifalian AM. Stem cells and cancer: an overview. Stem Cell Rev 2007;3:249–55.

5. Zou GM. Cancer stem cells in leukemia, recent advances. J Cell Physiol 2007; 213:440–4.

6. Li F, Tiede B, Massague J, Kang Y. Beyond tumorigenesis: cancer stem cells in metastasis. Cell Res 2007;17:3–14.

7. Screaton GR, Bell MV, Jackson DG, Cornelis FB, Gerth U, Bell JI. Genomic structure of DNA encoding the lymphocyte homing receptor CD44 reveals at least 12 alternatively spliced exons. Proc Natl Acad Sci U S A 1992;89:12160–4.

8. Lynch KW. Consequences of regulated pre-mRNA splicing in the immune system. Nat Rev Immunol 2004;4:931–40.

9. Ponta H, Sherman L, Herrlich P. CD44: from adhesion molecules to signalling regulators. Nat Rev Mol Cell Biol 2003;4:33–45.

10. Toole BP. Hyaluronan: from extracellular glue to pericellular cue. Nat Rev Cancer 2004;4:528–39.

11. Steeber DA, Venturi GM, Tedder TF. A new twist to the leukocyte adhesion cascade: intimate cooperation is key. Trends Immunol 2005;26:9–12.

12. Aruffo A, Stamenkovic I, Melnick M, Underhill CB, Seed B. CD44 is the principal cell surface receptor for hyaluronate. Cell 1990;61:1303–13.

13. Bourguignon LY, Zhu H, Shao L, Zhu D, Chen YW. Rho-kinase (ROK) promotes CD44(v3,8-10)-ankyrin interaction and tumor cell migration in metastatic breast cancer cells. Cell Motil Cytoskeleton 1999;43:269–87.

14. Tsukita S, Yonemura S, Tsukita S. ERM proteins: head-to-tail regulation of actin-plasma membrane interaction. Trends Biochem Sci 1997;22:53–8.

15. Oliferenko S, Kaverina I, Small JV, Huber LA. Hyaluronic acid (HA) binding to CD44 activates Rac1 and induces lamellipodia outgrowth. J Cell Biol 2000; 148:1159–64.

16. Lesley J, English NM, Gal I, Mikecz K, Day AJ, Hyman R. Hyaluronan binding properties of a CD44 chimera containing the link module of TSG-6. J Biol Chem 2002;277:26600–8.

17. Nandi A, Estess P, Siegelman M. Bimolecular complex between rolling and firm adhesion receptors required for cell arrest; CD44 association with VLA-4 in T cell extravasation. Immunity 2004;20:455–65.

18. Napier SL, Healy ZR, Schnaar RL, Konstantopoulos K. Selectin ligand expression regulates the initial vascular interactions of colon carcinoma cells: the roles of CD44v and alternative sialofucosylated selectin ligands. J Biol Chem 2007;282:3433–41.

19. Baronas-Lowell D, Lauer-Fields JL, Borgia JA, et al. Differential modulation of human melanoma cell metalloproteinase expression by $\alpha_2\beta_1$ integrin and CD44 triple-helical ligands derived from type IV collagen. J Biol Chem 2004; 279:43503–13.

20. Yu Q, Stamenkovic I. Transforming growth factor-β facilitates breast carcinoma metastasis by promoting tumor cell survival. Clin Exp Metastasis 2004;21:235–42.

21. Ghatak S, Misra S, Toole BP. Hyaluronan constitutively regulates ErbB2 phosphorylation and signaling complex formation in carcinoma cells. J Biol Chem 2005;280:8875–83.

22. Bourguignon LY, Zhu H, Zhou B, Diedrich F, Singleton PA, Hung MC. Hyaluronan promotes CD44v3-2 interaction with Grb2-185(HER2) and induces Rac1 and Ras signaling during ovarian tumor cell migration and growth. J Biol Chem 2001;276:48679–92.

23. Orian-Rousseau V, Chen L, Sleeman JP, Herrlich P, Ponta H. CD44 is required for two consecutive steps in HGF/c-Met signaling. Genes Dev 2002;16: 3074–86.

24. Marhaba R, Bourouba M, Zöller M. CD44v6 promotes proliferation by persisting activation of MAP kinases. Cell Signal 2005;17:961–73.

25. Ghatak S, Misra S, Toole BP. Hyaluronan oligosaccharides inhibit anchorage-independent growth of tumor cells by suppressing the phosphoinositide 3-kinase/Akt cell survival pathway. J Biol Chem 2002;277:38013–20.

26. Bourguignon LY, Singleton PA, Zhu H, Diedrich F. Hyaluronan-mediated CD44 interaction with RhoGEF and Rho kinase promotes Grb2-associated binder-1 phosphorylation and phosphatidylinositol 3-kinase signaling leading to cytokine (macrophage-colony stimulating factor) production and breast tumor progression. J Biol Chem 2003;278:29420–34.

27. Lee JL, Wang MJ, Sudhir PR, Chen GD, Chi CW, Chen JY. Osteopontin promotes integrin activation through outside-in and inside-out mechanisms: OPN-CD44V interaction enhances survival in gastrointestinal cancer cells. Cancer Res 2007;67:2089–97.

28. Marhaba R, Bourouba M, Zöller M. CD44v7 interferes with activation-induced cell death by up-regulation of anti-apoptotic gene expression. J Leukoc Biol 2003;74:135–48.

29. Matzku S, Komitowski D, Mildenberger M, Zöller M. Characterization of BSp73, a spontaneous rat tumor and its *in vivo* selected variants showing different metastasizing capacities. Invasion Metastasis 1983;3:109–23.

30. Matzku S, Werling HO, Waller C, Schmalenberger B, Zankl H. Clonal analysis of diversity in the BSp73 rat tumor. Invasion Metastasis 1985;5:356–70.

31. Matzku S, Wenzel A, Liu S, Zöller M. Antigenic differences between metastatic and nonmetastatic BSp73 rat tumor variants characterized by monoclonal antibodies. Cancer Res 1989;49:1294–9.

32. König H, Moll J, Ponta H, Herrlich P. Trans-acting factors regulate the expression of CD44 splice variants. EMBO J 1996;15:4030–9.

33. Duffy MJ, McGowan PM, Gallagher WM. Cancer invasion and metastasis: changing views. J Pathol 2008;214:283–93.

34. Cretu A, Brooks PC. Impact of the non-cellular tumor microenvironment on metastasis: potential therapeutic and imaging opportunities. J Cell Physiol 2007; 213:391–402.

35. Natarajan TG, FitzGerald KT. Markers in normal and cancer stem cells. Cancer Biomark 2007;3:211–31.

36. Neuzil J, Stantic M, Zobalova R, et al. Tumour-initiating cells vs. cancer 'stem' cells and CD133: what's in the name? Biochem Biophys Res Commun 2007;355:855–9.

37. Chambers AF, Groom AC, MacDonald IC. Dissemination and growth of cancer cells in metastatic sites. Nat Rev Cancer 2002;2:563–72.

38. Goswami A, Ranganathan P, Rangnekar VM. The phosphoinositide 3-kinase/Akt1/Par-4 axis: a cancer-selective therapeutic target. Cancer Res 2006; 66:2889–92.

39. Bates RC, Edwards NS, Burns GF, Fisher DE. CD44 survival pathway triggers chemoresistance via lyn kinase and phosphoinositide 3-kinase/Akt in colon carcinoma cells. Cancer Res 2001;61:5275–83.

40. Sohara Y, IshiguroN, Machida K, et al. Hyaluronan activates cell motility of v-Src-transformed cells via Ras-mitogen-activated protein kinase and phosphoinositide 3-kinase-Akt in a tumor-specific manner. Mol Biol Cell 2001; 12:1859–68.

41. Bourguignon LYW, Singleton P, Zhu H, Diedrich F. Hyaluronan-mediated. CD44 interaction with RhoGEF and Rho-kinase promotes Grb2-associated binding-1 phosphorylation and phosphatidylinositol 3-kinase signaling leading to cytokine (macrophage-colony stimulating factor) production and breast tumor progression. J Biol Chem 2003;278:29420–34.

42. Marhaba R, Freyschmidt-Paul P, Zöller M. *In vivo* CD44-49d complex formation in autoimmune disease has consequences on T cell activation and apoptosis resistance. Eur J Immunol 2006;36:3017–32.

43. Subramaniam V, Vincent IR, Gardner H, Chan E, Dhamko H, Jothy S. CD44 regulates cell migration in human colon cancer cells via Lyn kinase and AKT phosphorylation. Exp Mol Pathol 2007;83:207–15.

44. Lee JL, Wang MJ, Sudhir PR, Chen JY. CD44 engagement promotes matrix-derived survival through CD44-SRC-integrin axis in lipid rafts. Mol Cell Biol. Epub ahead of print 2008 Jul 21.

45. Kamikura DM, Khoury H, Maroun C, Naujokas MA, Park M. Enhanced transformation by a plasma membrane-associated met oncoprotein: activation of a phosphoinositide 3′-kinase-dependent autocrine loop involving hyaluronic acid and CD44. Mol Cell Biol 2000;20:3482–96.

46. Tulasne D, Foveau B. The shadow of death on the MET tyrosine kinase receptor. Cell Death Differ 2008;15:427–34.

47. Girish KS, Kemparaju K. Structure, evolution, and biology of the MUC4 mucin. FASEB J 2008;22:966–81.

48. Schmidt DS, Klingbeil P, Schnölzer M, Zöller M. CD44 variant isoforms associate with tetraspanins and EpCAM. Exp Cell Res 2004;297:329–47.

49. Shaw AR, Li L. Exploration of the functional proteome: lessons from lipid rafts. Curr Opin Mol Ther 2003;5:294–301.

50. Chen SY, Chen HC. Direct interaction of focal adhesion kinase (FAK) with Met is required for FAK to promote hepatocyte growth factor-induced cell invasion. Mol Cell Biol 2006;26:5155–67.

51. Menzel EJ, Farr C. Hyaluronidase and its substrate hyaluronan: biochemistry, biological activities and therapeutic uses. Cancer Lett 1998;131:3–11.

52. Fjeldstad K, Kolset SO. Decreasing the metastatic potential in cancers—targeting the heparan sulfate proteoglycans. Curr Drug Targets 2005;6:665–82.

53. Knudson CB. Hyaluronan and CD44: strategic players for cell-matrix interactions during chondrogenesis and matrix assembly. Birth Defects Res Part C Embryo Today 2003;69:174–96.

54. Stern R. Hyaluronan metabolism: a major paradox in cancer biology. Pathol Biol 2005;53:372–82.